Optics & Laser Technology 162 (2023) 109257

Contents lists available at ScienceDirect

Optics and Laser Technology

journal homepage: www.elsevier.com/locate/optlastec

Full length article

Sub-nanosecond, 41 mJ pulse energy, passively Q-switched Nd:YLF laser

Felipe Maia Prado, Tomás Junqueira Franco, Niklaus Ursus Wetter *

Lasers and Applications Center, Instituto de Pesquisas Energéticas e Nucleares, IPEN-CNEN, Av. Lineu Prestes 2242, São Paulo 05508-000, Brazil

ARTICLE INFO

Keywords:
Passive Q-switched
High energy
Nd:YLF crystal
Diode pumping
Sub-nanosecond

ABSTRACT

A sub-nanosecond, diode-stack side-pumped, passively Q-switched Nd^{3+}:YLF_4/Cr^{4+}:YAG Laser is reported in a compact cavity design, generating one pulse of 41 mJ with a pulse width of 894 ps, achieving a peak output power of 46 MW and beam quality M^2 of 5.4 × 5.9 (HxV). The number of pulses in the pulse train could be adjusted from one pulse to ten pulses of 111 mJ total output energy and 23.7 % optical efficiency by adjusting the focus distance while maintaining sub-nanosecond pulse duration. This resonator can also be used for high-power simultaneous Q-switched laser emission at 1047 nm and 1053 nm.

1. Introduction

Recent space missions such as the three rovers that arrived on Mars in 2020, namely NASA's Perseverance Rover [1], Emirate's Mars Mission (EMM) Hope Probe [2], and China's Tianwen-1 [3], indicate an increased interest in space exploration and the development of new and improved technologies in the field of Q-switched lasers. These laser systems have a wide range of spaceborne applications ranging from the use in analysis of the geophysical composition of planetary surfaces to tools such as Laser-Induced Breakdown Spectroscopy (LIBS) [4] and Laser-Desorption Mass Spectrometry (LDMS) as demonstrated in the European Space Agency's (ESA) ExoMars rover mission, which aimed to detect the presence of present and/or past life on Mars through the ionization of samples of large organic molecules on the surface and sub-surface of the planet [5] and to altimetry of planets and moons and distance measurements for purposes of docking and maneuvering [6]. Passively Q-switching lasers enable a more compact design, saving both mass and space, and allowing for a simpler cavity, less prone to electrical issues that are common in electro-optical or acousto-optical switches, thus reducing maintenance costs and increasing reliability. Saturable absorbers have also been demonstrated to withstand the harsh environment of space [4,6]. Highly energetic, short-pulsed, passively Q-switched lasers are also available for more classical laser applications such as advanced materials processing, laser shock peeling, high energy density (HED) physics studies, pump sources for other lasers, cutting, marking, and drilling [7], light detection and ranging (LIDAR), environmental monitoring [8] and medical applications in the fields of ophthalmology, dermatology, dentistry, and neurosurgery [9,10]. Shorter pulses also generate less residual heat, which diminishes possible damages and extra costs in fields such as laser processing and medical applications [11].

The most common neodymium doped crystals are Yttrium Aluminum Garnet (YAG), given its prominent mechanical and thermal properties, Yttrium Vanadate (YVO_4), and Gadolinium Vanadate ($GdVO_4$), for their natural birefringence that causes linearly polarized emission and very high absorption and emission cross-sections and Yttrium Lithium Fluoride ($LiYF_4$ or YLF) [12]. The latter presents a longer upper-state lifetime (~480 μs), which makes it suitable for high-energy pulses in Q-switched operation and diode-pumped lasers. Despite its low damage threshold (35 MPa), the crystal presents contributing factors to high-beam quality such as small birefringence and low-temperature variability of its index of refraction, along with weak thermal lensing when emitting at 1053 nm [12,13].

Longitudinal pumping schemes are often preferred for achieving high beam quality due to their optimal mode matching [14]. However, they require good spatial overlap between laser and pump beams incurring bulky and expensive fiber-coupled diode packaging when higher pump powers are required. A side-pumped configuration allows for scalability by the accumulation of multiple diodes (diode stacks) along the crystals' side facets and, additionally, avoids the pump bleaching effect, where the saturable absorber gets partially bleached by the pump beam, because the laser' optical axis and pump direction are orthogonal during side-pumping [12,15]. Furthermore, the geometrical focus obtained from the diode stack's emission has a rectangular shape with an aspect ratio that is conducive to efficient diode-side pumping, ensuring good spatial overlap without the need for fiber-coupling, while

* Corresponding author.
E-mail address: nuwetter.ipen@gmail.com (N. Ursus Wetter).

https://doi.org/10.1016/j.optlastec.2023.109257
Received 24 November 2022; Received in revised form 17 January 2023; Accepted 4 February 2023
Available online 19 February 2023

also being economical. Recent papers suggest that the efficiency of side-pumping configurations can surpass longitudinal pumping while still operating with high beam quality: A diffraction-limited, highly efficient beam was obtained in a side-pumped Nd:YLF double-bounce resonator and resulted in 65 % of slope and 63 % of optical efficiency when pumped at the four-level absorption transition close to 800 nm [16]. The result was achieved by employing two total internal reflections (TIR) of the laser beam at the pump face of the crystal thereby exposing the center of the TEM_{00} mode to the area of highest population inversion. This technique was dubbed double beam mode controlling (DBMC). In 2022 it was shown that side-pumped Nd:YLF lasers can achieve slope efficiencies as high as 68 % when pumped at 800 nm and 78 % with respect to incident pump power when direct pumping at 863 nm [17–19]. The latter was achieved using a symmetrical resonator with intracavity cylindrical lenses to obtain a near diffraction-limited output beam, and represents the highest efficiency ever reported for Nd:YLF and the second highest for any Nd laser.

The most common technique for obtaining highly-energetic short pulses is using a master oscillator power amplifier (MOPA). Although this approach is more efficient and can generate higher output powers and produce better quality beams at high output powers, it is also much more complex and expensive, heavier and bulkier, requiring multiple optical components and pump sources [6]. Active Q-switching can result in higher efficiency as it avoids energy loss due to residual absorption of saturated passive Q-switching and also has less timing jitter allowing for the precise temporal release of the Q-switched pulse. Using an electro-optical modulator in a diode side-pumped Nd:YLF laser, a pulse energy of 160 mJ with a pulse width of 9 ns was achieved in an output beam with a M^2 of 8.39 × 7.37, vertically and horizontally, respectively [20]. If single-pulse, quasi-continuous (QCW) pumping is used in passively Q-switched lasers, the timing jitter is smaller by orders of magnitude when compared to continuous-wave (CW) pumping, making it comparable to active Q-switching [16,21]. MOPA laser designs do not exclusively rely on active Q-switching and for some applications, the master oscillator is passively Q-switched. In a MOPA laser system, using a passive Cr:YAG absorber together with a Nd:YAG crystal to fabricate a linearly polarized seed laser, a 600 mJ output energy and a 420 ps pulse width were achieved while maintaining a M^2 value of 1.17 [22].

The most compact diode-pumped solid-state lasers are microchip lasers. Q-switched microchip lasers generate short high-energy pulses for various industrial applications while maintaining a lightweight and cheap cavity design [23]. However, their compact cavity restricts the size of the gain medium, limiting their peak-energy output. In 2021 Lim and Taira demonstrated a Q-switched microchip laser in a Nd:YAG/Cr^{4+}:YAG unstable resonator generating pulses of 17 mJ with a duration of 452 ps, which corresponded to a peak power of 37.6 MW for Q-switched Nd lasers [24].

Standard Q-switches with lower initial transmission result in higher residual losses, decreasing the slope efficiency and limiting pulse energy [25]. The optimal solution is to find a balance between the initial transmission and residual loss, resulting in an optimization of the output energy. In 2013, a diode side-pumped Nd:YLF laser passively Q-switched by a Cr:YAG crystal achieved pulse energies of 23 mJ and 19 mJ at the σ- and π-transition, respectively, with a 9 ns pulse width, thus a maximum output power of 2.5 MW, with M^2 values of 3.5 and 5.5 in the vertical- and horizontal directions, respectively [26]. Higher single-pulse energies were reported for a passively Q-switched Nd:YAG laser in a resonator longitudinally diode-pumped with 3000 W generating pulse energy of 40 mJ, 18 ns pulse width, and 2.2 MW peak output power by passively Q-switching with a Cr:YAG of 70 % initial absorption [25]. In another Nd:YAG/Cr:YAG configuration, side-pumped by 3880 W, 53 mJ of output pulse energy and 10.4 ns pulse width were achieved (5.5 MW of peak output power) while presenting a M^2 value of 9 [27], representing the highest reported energy for diode-pumped passively Q-switched Nd lasers disregarding MOPA configurations.

In this work, we present a 797 nm diode side-pumped, passively Q-switched Nd:YLF/Cr:YAG laser emitting at 1047 nm. This configuration produced a pulse energy of 41.25 mJ with 894.02 ps of duration, resulting in a peak output power of 46.14 MW and the highest pulse energy value for a diode-pumped passively Q-switched Nd:YLF laser. The beam had M^2 values of 5.9 × 5.4 in the vertical and horizontal direction, respectively, which fares well when compared to similar configurations.

2. Experimental design

Prior to laser operation simulations were made to ensure that the host material could withstand the power output of the diode stack. The programs used were a commercial program (LASCAD version 3.6), which applies a finite element analysis for solid-state laser cavity evaluation and design, and a MatLab script simulating the effects in temperature and stress of a QCW pumped Nd:YLF crystal based on the theory of Bernhardi et al., which analyses the thermally induced stress in Nd:YLF lasers [28]. It was found that the maximum thermally induced shear stress, obtained at the center of the upper edge of the crystal's pump facet, was 15 MPa, which is less than half of its damage threshold of 35 MPa, indicating that it should be safe to use the crystal at the pump parameters given below. Furthermore, it was determined that there was very little residual heat build-up between pulses, suggesting that along with a cooling system, the laser could be operated for long periods. Both, pump laser and crystal were water cooled. A 12-bar, fast-axis collimated and VBG (volume Bragg grating) equipped diode-stack (Northrop Grumman, US), with a measured peak power of 1470.36 ± 2.86 W, emitting at 797 nm was used to side-pump an a-cut Nd:$YLiF_4$ crystal containing 1 mol% Nd^{3+} doping (Crystech, China) with dimensions of 13 mm × 13 mm × 3 mm (LxWxH). The pump laser was operated with a pulse duration of 346.5 ± 0.53 μs and a repetition rate of 5 Hz. Both duty cycle and peak pump power had to be maintained for optimal narrowing of the 797 nm emission line by the VBG (measured linewidth of 0.92 ± 0.03 nm at FWHM).

In order to achieve only one Q-switched laser pulse for each pump pulse of the diode laser, the crystal was placed in a single-bounce resonator, with a total length of 63 mm, consisting of two mirrors (Layertec, DE), one highly reflective (HR) concave mirror with 10 m of radius of curvature (M2) and one flat output coupler (M1) with 70 % transmission which was optimized for this laser during experimentation with several combinations (mirrors of 96 %, 70 %, 50 %, 30 %, 20 %, 15 % and 10 % transmission and absorbers of 1 %, 4 % 10 %, 20 % 30 % and 60 % initial transmission). The highest single pulse energy was achieved for a Cr:YAG passive absorber (Foctek, CN) with 10 % initial transmission (QS1). The resonator configuration employs a Brewster angle incidence (55.4° for the σ-transition) at the lateral facets of the crystal to achieve lossless 1053 nm transmission, in QCW operation, of the σ-polarized light into and out of the gain medium while undergoing a total internal reflection (TIR) at the pump facet of the crystal, as shown in Fig. 1.

Normally, tight pump focusing is required to achieve maximum gain of the laser. This increase in gain has to be compensated by a higher saturable absorption, which in turn increases the non-saturable losses of the absorber. The best compromise between losses and gain, resulting in the highest pulse energy, was experimentally found by substituting the traditional f = 40 mm pump lens with a 75 mm biconvex lens (SL). After the lens, a λ/2 waveplate (HP) was inserted to rotate the polarization of the pump beam to coincide with the absorption peak of the π-polarization along the c-axis. The incident power on the surface of the crystal, after focusing the diode beam, was 1406.4 ± 2.7 W (487.3 ± 0.6 mJ), representing a coupling efficiency of 95.65 ± 1.4 %, mainly due to the lack of an AR coating at the pump face of the crystal. To reduce energy loss due to amplified spontaneous emission (ASE), which was strong, parallel, and close to the pump face as well as between the pump facet and the opposite back facet, the border of the back facet was clipped at an angle and one of the crystal's side facet borders was also clipped close

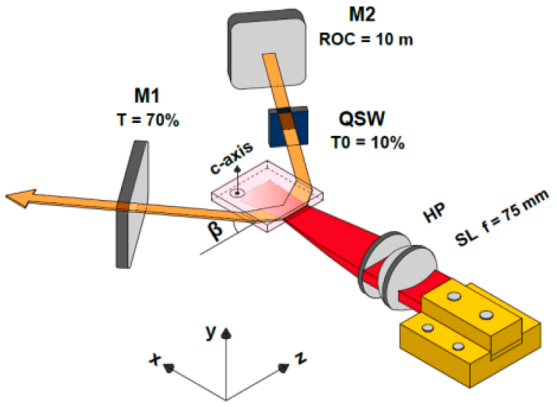

Fig. 1. Passively Q-switched resonator design. M1 is an output coupler with 70 % transmission; M2 is a HR mirror with 10 m of radius of curvature (ROC); QSW is a saturable absorber with 10 % transmission; HP is a half waveplate; SL is a biconvex spherical lens with f = 75 mm and β is the Brewster angle.

to the corner with the pump facet. This procedure effectively disabled the creation of an internal resonator and eliminated ASE.

3. Results and discussion

3.1. Quasi-CW operation

We first optimized the resonator without a saturable absorber. Using a 25 mm lens, a 20 % transmission flat output coupler, and one HR concave mirror with a 3 m radius of curvature, a peak output power of 879.5 ± 24.8 W and a slope efficiency of 67.2 ± 0.4 % were obtained, with an optical-to-optical efficiency of 64.4 ± 2.2 %, as demonstrated in Fig. 2. The latter represents the record slope efficiency for a Nd:YLF laser pumped at the traditional absorption band at 800 nm and is in agreement with recent results of the same side-pumped configuration published by our group [16–19]. Next, we optimized the resonator with the saturable absorber inside in terms of Q-switched pulse energy, which resulted in the cavity of Fig. 1, explained in item 2. Without the saturable absorber, the peak output power for this laser was 496.5 ± 17.7 W, resulting in an optical-to-optical efficiency of 36.3 ± 1.8 % and a slope efficiency of 41.0 ± 0.6 %.

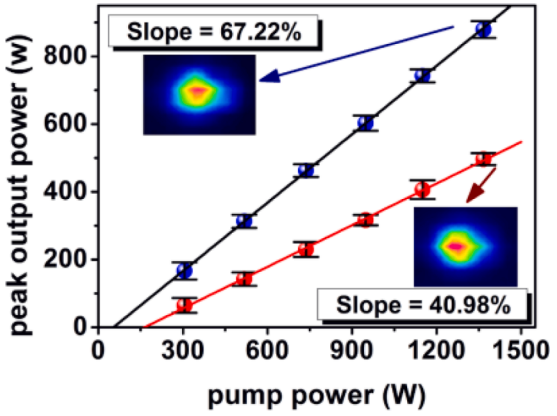

Fig. 2. Slope efficiency diagram of the laser resonator in QCW operation without a saturable absorber, with respect to the absorbed pump power (which is equal to incident pump power minus 3.6 % Fresnel losses from the uncoated Nd:YLF crystal). The red points indicate the slope efficiency with a HR mirror of 10 m, an output coupler of T = 70 %, and a SL of 75 mm, resulting in a slope efficiency of 41.0 ± 0.6 %. The blue points indicate the slope efficiency, using a HR mirror of 3 m, an output coupler of T = 20 %, and a SL of 25 mm, resulting in a slope efficiency of 67.2 ± 0.4 %. Inset: Beam profile captured by a Newport LBP series beam profiler.

3.2. Single *Q-switched pulse*

The number of Q-switched pulses per pump pulse was controlled changing the pump spot size by moving the focusing lens. The maximum output energy for a single Q-switched pulse was obtained for only one Q-switched pulse within the pump pulse duration. This situation occurred when the 75 mm spherical lens created a focal spot size of 5.11 ± 0.07 mm and 1.01 ± 0.02 mm along the horizontal and vertical axis, respectively. The single Q-switched pulse occurred at the end of the pump cycle with an output energy of 41.3 ± 0.2 mJ (Coherent, model Field Max II energy meter). This result could be easily reproduced even after four months of daily operation and remained stable with low fluctuations, as shown in Fig. 3A. The recorded pulse width of 945.6 ± 10.4 ps (LeCroy Wave Runner 104MXi Oscilloscope of 1 GHz and 10GS/s with a rise time of 300 ps, and Thorlabs InGaAs Biased Detector, model DET08CFC, of 5 GHz with a rise time of 70 ps) was obtained as a mean of 4 pulse traces, each being the average of 25 single pulse traces of the oscilloscope.

The measured pulse width is the result of a convolution of the real pulse width with the response times of the photodetector and the oscilloscope [29,30]. The real pulse width was calculated to be 894.02 ± 11.03 ps, resulting in a peak power of 46.14 ± 0.59 MW. The sub-nanosecond pulse duration was mainly a consequence of the compact cavity, an advantage of saturable absorbers in comparison with their active counterparts. In 2019, a similar configuration employing the same crystals achieved a single pulse of 750 ps and 2.3 mJ resulting in a peak power of 3 MW [30]. Disregarding values reported by MOPA systems, this result represents the highest peak power ever reported for a diode-pumped passively Q-switched Nd:YLF laser, furthermore, its pulse energy of 41 mJ also represents the highest value ever achieved for the combination Nd:YLF/Cr:YAG. As shown in Fig. 3B, the average Q-switched pulse occurred at 343 μs (Rigol DS4034 digital oscilloscope of 350 MHz and 4GSa/s) after the start of the pump pulse. The timing jitter of the Q-switched laser had a standard deviation of only 1.53 μs, which is small enough for many applications that require triggering. The optical-to-optical efficiency of the Q-switched resonator was 8.46 ± 0.03 %. The stability diagram in Fig. 3A and the fact that the resonator could be operated for months without changing noticeably its pulse energy show that the residual heat is neither an issue in the crystal nor in the saturable absorber, which enriches the possibilities of applications with this design. Compared to the works cited in the introduction, the pump coupling efficiency of 96 % was significantly higher than the 55 % employed in the longitudinal-pumping scheme used to achieve pulse energy of 40 mJ [25] and our optical efficiency of 8.46 % also fares well against the ~ 10 % achieved in the side-pumped configuration that resulted in the highest pulse energy, of 53 mJ, ever reported by a passively Q-switched Nd laser, without being a MOPA configuration [27].

Shown in Fig. 4 are the M^2 values of the Q-switched pulse of 5.87 ±

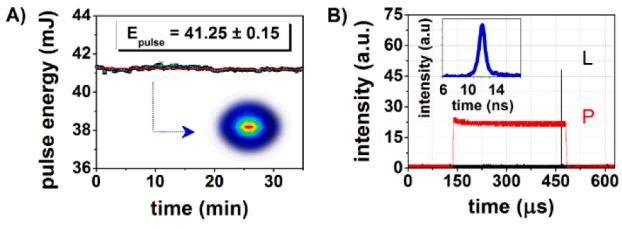

Fig. 3. A: Energy stability diagram. Each measurement point corresponds to the average of 125 pulses taken every 25 s throughout 35 min of laser operation, resulting in an average pulse energy of 41.25 ± 0.15 mJ. The fit (red line) presented a residual standard deviation (STD) of 0.08 mJ. The inset represents the beam profile of the Q-switched pulse, captured by a Newport LBP series beam profiler. B: Oscilloscope traces of the pump pulse (P) and Q-switched laser pulse (L) in arbitrary units (a.u.). The inset shows an oscilloscope trace of the single Q-switched pulse of 945 ps in arbitrary units (a.u.).

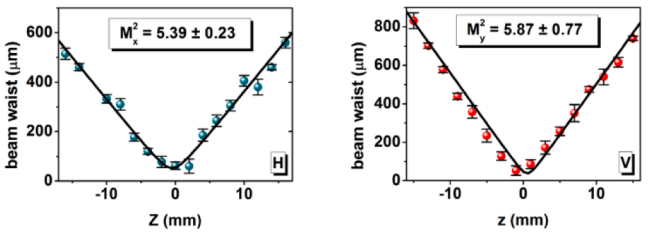

Fig. 4. Beam waist measurements of the Q-switched pulse in the horizontal (H) and vertical (V) directions. The fitted curves presented a residual standard deviation of 10.88 μm and 14.73 μm in the V- and H- directions, respectively.

0.77 and 5.39 ± 0.23 in the vertical- and horizontal directions, respectively; the values were obtained with a non-linear fit of the data collected employing the knife edge technique [31].

The measured M^2 values fare well when compared to the other side-pumping Q-switched lasers already mentioned, such as the M^2 of 9 achieved by the passively Q-switched Nd:YAG laser with 53 mJ of pulse energy of reference [27] or the M^2 of 8 achieved by the actively Q-switched Nd:YLF laser that produced 160 mJ of pulse energy [20].

Laser emission without a saturable absorber occurred only at the σ-transition, due to the smaller gain and the losses introduced by the Brewster angle of incidence (see Fig. 1). With a saturable absorber, the Q-switched laser emitted at the 1047 nm wavelength of higher emission cross-section (approx. 30 % higher than 1053 nm emission cross-section). The higher gain during Q-switched operation strongly dominates over losses and the laser operated even with a 96.4 % output coupler. Fig. 5 shows the spectrum of the laser emission under Q-switched and QCW operations.

With regard to the more compact microchip lasers, capable of achieving smaller pulse widths [24], our design generates much higher pulse energy and very high peak powers. Femtosecond lasers can easily reach even higher peak powers due to their extremely short pulse widths, but are fairly limited regarding their pulse energy when compared to this work, are much bulkier and require much higher investment costs [32].

3.3. *Multiple* ***Q-switched pulses***

Whereas the resonator of Fig. 1 was optimized to generate the emission of one single, high-energy Q-switched pulse, it is also possible to achieve pulse trains, within the same setup and using the same pump parameters, simply changing the pump spot size on the Nd:YLF by moving the focusing lens in the direction of the crystal. Fig. 6A, B, and C present the pulse trains with 8, 4, and 2 Q-switched pulses per pump pulse, the inset displays an oscilloscope trace of each configuration with average pulse widths of 917.7 ± 14.8 ps, 950.8 ± 11.9 ps, and 930.0 ± 11.6 ps, respectively.

Fig. 6D shows the energy per pulse versus the number of Q-switched pulses in the pulse train for different pump powers. Three different incident peak pump powers of 1406.4 ± 2.7 W, 1182.5 ± 3.2 W, and 975.1 ± 2.6 W were achieved maintaining the emission wavelength and a linewidth of less than 1 nm by elevating the diode's operating

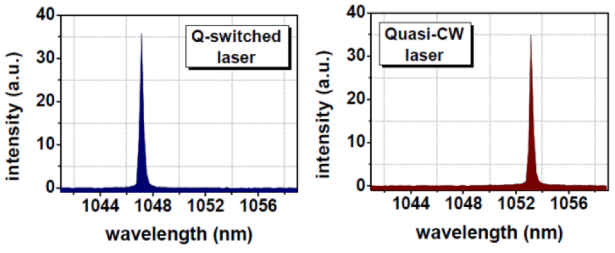

Fig. 5. Spectrum of the laser emission in the Q-switched and QCW regime.

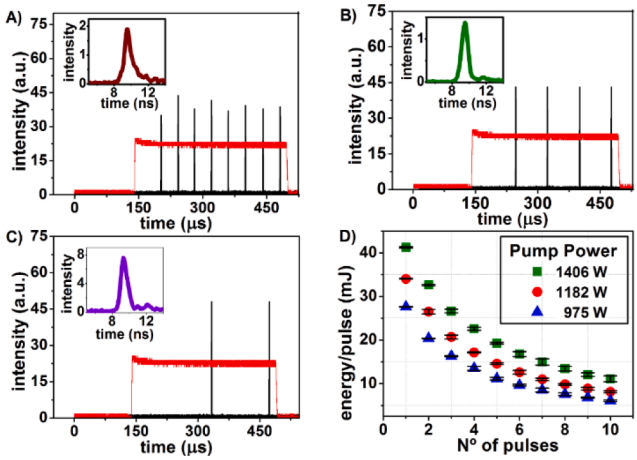

Fig. 6. A, B, and C: Pulse trains of the Q-switched laser for different pump spot sizes, produced by a 75 mm spherical lens, at maximum pumping power. The insets show an oscilloscope trace of the Q-switched pulses in each pulse train in arbitrary units (a.u.). D: Energy per pulse versus the N° of pulses in the pulse train. Each curve indicates a different peak pump power used in the laser cavity (squares = 1406 W; circles = 1182 W; triangles = 975 W).

temperature up to less than 35 °C. The maximum number of pulses obtained was 10 during a single pump duration. The highest energy for a single pulse was 41 mJ and for ten pulses 111.1 ± 7.0 mJ. The latter result corresponds to an optical-to-optical efficiency of 23.7 ± 0.2 % under Q-switched operation.

To achieve a certain number of Q-switched pulses in the pulse train, the pump cross-sections on the pump face of the Nd:YLF was changed by moving the focus of the 75 mm spherical lens. The pump areas used to achieve a single Q-switched pulse for the incident pump powers of 1406 W, 1182 W, and 975 W were 4.0 ± 0.1 mm^2, 3.7 ± 0.1 mm^2, and 2.4 ± 0.1 mm^2, respectively. To emit a pulse train with 10 Q-switched pulses the areas used to pump the Nd:YLF were 1.84 ± 0.04 mm^2, 1.96 ± 0.04 mm^2, 2.02 ± 0.06 mm^2, for the pump powers of 1406 W, 1182 W, and 975 W, respectively.

The measured pulse widths, for each of the experimental points presented in Fig. 6D, remained similar for all configurations despite the variations of pump energy and pump spot size, presenting an STD of 31.41 ps with a corrected mean pulse width of 876.06 ps. This is the average of all pulses of the train and not only the first pulses shown in the insets of Fig. 6.

Fig. 7 displays the peak output power of some of the best results for

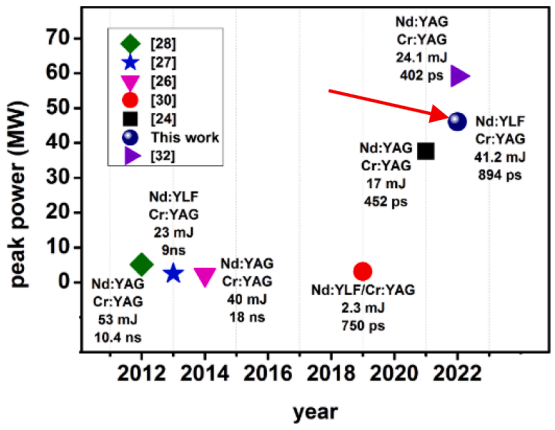

Fig. 7. Peak output power of some of the best results of passively Q-switched lasers encountered in the literature (MOPA configurations excluded). Indicated are the pulse width, the pulse energy, the active medium, and the saturable absorber of the respective laser. The inset lists the respective references.

passively Q-switched lasers encountered in the literature (MOPA configurations excluded). During the writing of this manuscript, we have become aware that recently a higher peak output power has been achieved with a microchip Nd:YAG/Cr:YAG unstable cavity [33], which is, to our knowledge, the only other result of a neodymium passively (non-MOPA) Q-switched laser with higher peak output power.

3.4. *Dual-wavelength* **Q-switched emission**

As explained in 3.2, for very high inversion densities (high pulse energies) the laser emission occurred at the 1047 nm wavelength despite the Brewster angle of incidence for the σ-transition at the Nd:YLF side-facets, which indicates that there must be a transition from the π to the σ polarization if we lower the pulse gain, allowing simultaneous dual-wavelength emission. By decreasing the saturable absorber's initial transmission to 60 % (lower inversion) and adjusting the mirror transmission to 80 % in the cavity of Fig. 1, we achieved simultaneous 1047 nm and 1053 nm operation in a pulse train with four Q-switched laser pulses and total output energy of 74.26 ± 1.37 mJ (~51.29 mJ at 1053 nm, and ~ 22.97 mJ at 1047 nm), as shown in Fig. 8A.

Pulse width of both wavelengths was 3.25 ± 0.08 ns at 1047 nm, and 6.2 ± 0.19 ns at 1053 nm. Fig. 8B displays the oscilloscope trace of the dual laser emission. Fig. 8C and 8D are captured by positioning a linear polarizer, with the respective orientation between the laser output and the fast detector. Fine-tuning of the losses incurring to the σ -emission was achieved by adjusting the incidence angle at the crystal's side-facet close to the Brewster's angle. This tuning determined not only the ratio of σ to π output pulse energy but also the delay of the σ pulse with respect to the π pulse, which could be adjusted from zero delay to several tens of nanoseconds as shown in Fig. 8B.

4. Conclusion

A passively Q-switched Nd:YLF/Cr:YAG resonator, with a total internal reflection at the pump face, side-pumped at 797 nm by a 12-bar diode stack and emitting at 1047 nm, achieved single pulse energy of 41 mJ and pulse duration of 894 ps resulting in 46.14 MW of peak power, which is the highest output power reported for a passively Q-switched single Nd:YLF oscillator. The laser beam had an M^2 of 5.39 in the horizontal, and 5.87 in the vertical direction. The small footprint of this laser resonator and the high pulse energy make this cavity an excellent candidate for a wide range of applications such as drones for pollution measurements and rovers for space exploration. Other interesting characteristics presented by this compact cavity are easy and precise determination of the number of emitted Q-switched pulses by control of a single parameter (distance of focusing lens to crystal), allowing for a smooth transition from 1 pulse of 41 mJ to ten pulses of 111 mJ total energy, and the possibility of generating simultaneous dual-wavelength emission at 1047 nm and 1053 nm, which is of interest to THz applications, amongst other, especially at these high output powers and relatively short pulse durations.

Funding

We thank the Comissão Nacional de Energia Nuclear (CNEN) [grant n° 01342.002132/2020-7], the Fundação de Amparo à Pesquisa do Estado de São Paulo (FAPESP) [2017/10765-5] and the Conselho Nacional de Desenvolvimento Científico e Tecnológico (CNPq)[465763/2014-6; 308526/2021-0].

CRediT authorship contribution statement

Felipe Maia Prado: Methodology, Validation, Formal analysis, Investigation, Writing – review & editing, Visualization. **Tomás Junqueira Franco:** Software, Formal analysis, Investigation, Data curation, Writing – original draft. **Niklaus Ursus Wetter:** Conceptualization, Methodology, Validation, Software, Resources, Supervision, Project administration, Funding acquisition, Writing – review & editing, Visualization.

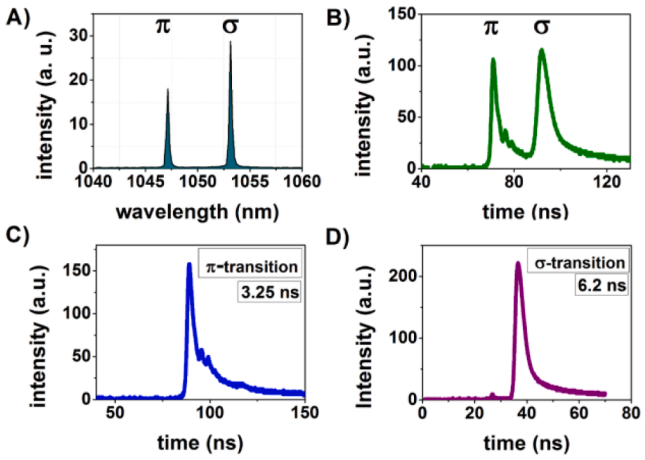

Fig. 8. A: Spectrogram of the dual-wavelength laser emission. B: Oscilloscope trace. C and D: Oscilloscope traces of the 1047 nm and 1053 nm emissions, respectively, obtained by positioning a linear polarizer in the vertical and horizontal direction, respectively.

Declaration of Competing Interest

The authors declare the following financial interests/personal relationships which may be considered as potential competing interests: Niklaus Ursus Wetter reports financial support was provided by State of Sao Paulo Research Foundation. Niklaus Ursus Wetter reports financial support was provided by National Council for Scientific and Technological Development. Felipe Maia Prado reports financial support was provided by Brazilian Nuclear Energy Commission.

Data availability

Data will be made available on request.

References

[1] J.N. Maki, D. Gruel, C. McKinney, M.A. Ravine, M. Morales, D. Lee, R. Willson, D. Copley-Woods, M. Valvo, T. Goodsall, J. McGuire, R.G. Sellar, J.A. Schaffner, M. A. Caplinger, J.M. Shamah, A.E. Johnson, H. Ansari, K. Singh, T. Litwin, R. Deen, A. Culver, N. Ruoff, D. Petrizzo, D. Kessler, C. Basset, T. Estlin, F. Alibay, A. Nelessen, S. Algermissen, The Mars 2020 Engineering Cameras and Microphone on the Perseverance Rover: A Next-Generation Imaging System for Mars Exploration, Space Sci. Rev. 216 (8) (2020) 1–48, https://doi.org/10.1007/s11214-020-00765-9.

[2] H.E.S. Amiri, D. Brain, O. Sharaf, P. Withnell, M. McGrath, M. Alloghani, M. Al Awadhi, S. Al Dhafri, O. Al Hamadi, H. Al Matroushi, Z. Al Shamsi, O. Al Shehhi, M. Chaffin, J. Deighan, C. Edwards, N. Ferrington, B. Harter, G. Holsclaw, M. Kelly, D. Kubitschek, B. Landin, R. Lillis, M. Packard, J. Parker, E. Pilinski, B. Pramman, H. Reed, S. Ryan, C. Sanders, M. Smith, C. Tomso, R. Wrigley, H. Al Mazmi, N. Al Mheiri, M. Al Shamsi, E. Al Tunaiji, K. Badri, P. Christensen, S. England, M. Fillingim, F. Forget, S. Jain, B.M. Jakosky, A. Jones, F. Lootah, J.G. Luhmann, M. Osterloo, M. Wolff, M. Yousuf, T.E.M. Mission, Space Sci. Rev. 218 (1) (2022) 1–46, https://doi.org/10.1007/s11214-021-00868-x.

[3] X. Tan, J. Liu, X. Zhang, W. Yan, W. Chen, X. Ren, W. Zuo, C. Li, Design and Validation of the Scientific Data Products for China's Tianwen-1 Mission, Space Sci. Rev. 217 (5) (2021) 1–22, https://doi.org/10.1007/s11214-021-00843-6.

[4] T. Lang, D. Kracht, J. Neumann, R. Huss, M. Ernst, A. Moalem, C. Kolleck, Development of a pulsed laser system for laser-induced breakdown spectroscopy (LIBS), SPIE-Intl Soc Optical Eng (2017) 655–660, https://doi.org/10.1117/12.2309093.

[5] C. Kolleck, M. Ernst, M. Hunnekuhl, A. Moalem, D. Kracht, J. Neumann, A. Büttner, M. Priehs, T. Hülsenbusch, Enhancement of the design of a pulsed UV laser system for a laser-desorption mass spectrometer on Mars, SPIE-Intl Soc Optical Eng (2018) 346–351, https://doi.org/10.1117/12.2309097.

[6] D. Kracht, J. Neumann, R. Huss, C. Kolleck, Energy scaling of passively Q-switched lasers In the Mj-range, SPIE-Intl Soc Optical Eng (2017) 1446–1448, https://doi.org/10.1117/12.2304075.

[7] K. Washio, Neodymium-doped solid-state lasers and their applications to materials processing, Mater. Chem. Phys. 31 (1–2) (1992) 57–66, https://doi.org/10.1016/0254-0584(92)90153-Y.
[8] V.M. Polyakov, V.V. Vitkin, D.I. Lychagin, A.A. Krylov, V.A. Buchenkov, S. V. Kashcheev, Compact Q-switched high repetition rate Nd:YLF laser with 100 mJ pulse energy for airborne lidars, in: Proc. - 2014 Int. Conf. Laser Opt. LO, IEEE Computer Society, 2014, pp. 1–2, https://doi.org/10.1109/LO.2014.6886233.
[9] C.Y. Mardin, R.P. Tornow, F.E. Kruse, Lasers in ophthalmology, Phys. Procedia 5 (2010) 631–636, https://doi.org/10.1016/j.phpro.2010.08.091.
[10] Q. Peng, A. Juzeniene, J. Chen, L.O. Svaasand, T. Warloe, K.E. Giercksky, J. Moan, Lasers in medicine, Reports Prog. Phys. 71 (5) (2008), 056701, https://doi.org/10.1088/0034-4885/71/5/056701.
[11] Q. He, B. Zhang, Z. Jiao, Short-Pulse Nd: YAG/Cr: YAG Microchip Laser With Pulse Duration of< 200 ps, IEEE Photon. Technol. Lett. 34 (14) (2022) 717–720, https://doi.org/10.1109/LPT.2022.3183024.
[12] N.U. Wetter, E.C. Sousa, F.D.A. Camargo, I.M. Ranieri, S.L. Baldochi, Efficient and compact diode-side-pumped Nd:YLF laser operating at 1053nm with high beam quality, J. Opt. A Pure Appl. Opt. 10 (10) (2008), 104013, https://doi.org/10.1088/1464-4258/10/10/104013.
[13] H. Zhang, D. Li, P. Shi, R. Diart, A. Shell, C.R. Haas, K. Du, Efficient, high power, Q-switched Nd:YLF slab laser end-pumped by diode stack, Opt. Commun. 250 (1–3) (2005) 157–162, https://doi.org/10.1016/j.optcom.2005.02.001.
[14] Z. Sedaghati, M. Nadimi, A. Major, Efficient continuous-wave Nd:YLF laser in-band diode-pumped at 908 nm and its thermal lensing, Laser Phys. Lett. 16 (12) (2019), 125002, https://doi.org/10.1088/1612-202X/ab5a85.
[15] J.J. Zayhowski, A.L. Wilson, Pump-Induced Bleaching of the Saturable Absorber in Short-Pulse Nd:YAG/Cr4+:YAG Passively Q-Switched Microchip Lasers, IEEE J. Quantum Electron. 39 (12) (2003) 1588–1593, https://doi.org/10.1109/JQE.2003.819535.
[16] N.U. Wetter, A.M. Deana, Influence of pump bandwidth on the efficiency of side-pumped, double-beam mode-controlled lasers: establishing a new record for Nd: YLiF_4 lasers using VBG, Opt. Express 23 (7) (2015) 9379–9387, https://doi.org/10.1364/oe.23.009379.
[17] F.M. Prado, N.U. Wetter, Nd:YLF laser pumped at 797 nm with 68% slope efficiency, SPIE-Intl Soc. Optical Eng. (2022) 28–32, https://doi.org/10.1117/12.2608967.
[18] T. de A. Vieira, F.M. Prado, N.U. Wetter, Nd:YLF laser at 1053 nm diode side pumped at 863 nm with a near quantum-defect slope efficiency, Opt. Laser Technol. 149 (2022), 107818, https://doi.org/10.1016/j.optlastec.2021.107818.
[19] F. Prado, T. Franco, T. Vieira, N. Wetter, High power Nd:YLF four-level lasers with 68% slope efficiency, Appl Opt (2023), https://doi.org/10.1364/AO.476541.
[20] Q. Yang, J. Ma, T. Lu, X. Ma, X. Zhu, 160mJ and 9ns electro-optics Q-switched conductively cooled 1047nm Nd:YLF laser, in: XX Int. Symp. High-Power Laser Syst. Appl. 2014, SPIE (2015), 64-73. DOI: https://doi.org/10.1117/12.2064316.
[21] A.M. Deana, I.M. Ranieri, S.L. Baldochi, N.U. Wetter, Compact, diode-side-pumped and Q-switched Nd:YLiF 4 laser cavity operating at 1053 nm with diffraction limited beam quality, Appl. Phys. B Lasers Opt. 106 (4) (2012) 877–880, https://doi.org/10.1007/s00340-011-4828-1.
[22] H.C. Lee, D.W. Chang, E.J. Lee, H.W. Yoon, High-energy, sub-nanosecond linearly polarized passively Q-switched MOPA laser system, Opt. Laser Technol. 95 (2017) 81–85, https://doi.org/10.1016/j.optlastec.2017.04.024.
[23] E. Molva, Microchip lasers and their applications in optical microsystems, Opt. Mater. 11 (2–3) (1999) 289–299, https://doi.org/10.1016/S0925-3467(98)00050-0.
[24] H. Hong Lim, T. Taira, 37 MW peak power unstable resonator microchip laser, in: Advanced Solid State Lasers, Optical Society of America, 2021, p. JTu1A. 21., https://doi.org/10.1364/ASSL.2021.JTu1A.21.
[25] M. W. Smillie, M. Silver, S. T. Lee, T. J. Cook, High single-pulse energy, passively Q-switched Nd:YAG laser for defence applications, in: Solid State Lasers XXIII Technol. Devices, SPIE (2014), 89590Z. https://doi.org/10.1117/12.2036934.
[26] C.Y. Cho, Y.P. Huang, Y.J. Huang, Y.C. Chen, K.W. Su, Y.F. Chen, Compact high-pulse-energy passively Q-switched Nd:YLF laser with an ultra-low-magnification unstable resonator: application for efficient optical parametric oscillator, Opt. Express 21 (2) (2013) 1489–1495, https://doi.org/10.1364/OE.21.001489.
[27] K. Lee, H.C. Lee, J.Y. Cho, J.C. Lee, J. Yi, Passively Q-switched, high peak power Nd:YAG laser pumped by QCW diode laser, Opt. Laser Technol. 44 (7) (2012) 2053–2057, https://doi.org/10.1016/j.optlastec.2012.03.027.
[28] E.H. Bernhardi, A. Forbes, C. Bollig, M.J.D. Esser, Estimation of thermal fracture limits in quasi-continuous-wave end-pumped lasers through a time-dependent analytical model, Opt. Express 16 (2008) 11115–11123, https://doi.org/10.1364/OE.16.011115.
[29] P.R. Bolton, Measurement and Deconvolution of Detector Response Time for Short Pulses, Lawrence Livermore National Laboratory, CA (USA) (1987), https://doi.org/10.2172/6289252.
[30] R.S. Cudney, C.E. Minor, Sub-nanosecond, megawatt compact diode-pumped Nd: YLF laser, Rev. Mex. de Fis. 64 (5) (2018) 512–518, https://doi.org/10.31349/RevMexFis.64.512.
[31] A.E. Siegman, Choice of Clip Levels for Beam Width Measurements Using Knife-Edge Techniques, IEEE J. Quantum Electron. 27 (4) (1991) 1098–1104, https://doi.org/10.1109/3.83346.
[32] J. Brons, High-power femtosecond laser-oscillators for applications in high-field physics, Ludwig Maximilians Universität München, 2017. Doctoral dissertation.
[33] H.H. Lim, T. Taira, >50 MW peak power, high brightness Nd:YAG/Cr4+:YAG microchip laser with unstable resonator, Opt. Express 30 (2022) 5151–5158, https://doi.org/10.1364/OE.450335.